5-Diphosphoinositol pentakisphosphate (5-IP$_7$) regulates phosphate release from acidocalcisomes and yeast vacuoles

Received for publication, September 15, 2018, and in revised form, October 10, 2018 Published, Papers in Press, October 12, 2018, DOI 10.1074/jbc.RA118.005884

Evgeniy Potapenko[‡§1], Ciro D. Cordeiro[‡§1], Guozhong Huang[‡], Melissa Storey[‡], Christopher Wittwer[¶], Amit K. Dutta[¶], Henning J. Jessen[¶], Vincent J. Starai[‖], and Roberto Docampo[‡§2]

From the [‡]Center for Tropical and Emerging Global Diseases and the Departments of [§]Cellular Biology and [‖]Microbiology and Infectious Diseases, University of Georgia, Athens, Georgia 30602 and the [¶]Department of Chemistry and Pharmacy, University of Freiburg, 79098 Freiburg, Germany

Edited by Ursula Jakob

Acidocalcisomes of *Trypanosoma brucei* and the acidocalcisome-like vacuoles of *Saccharomyces cerevisiae* are acidic calcium compartments that store polyphosphate (polyP). Both organelles possess a phosphate–sodium symporter (TbPho91 and Pho91p in *T. brucei* and yeast, respectively), but the roles of these transporters in growth and orthophosphate (P_i) transport are unclear. We found here that *Tbpho91*$^{-/-}$ trypanosomes have a lower growth rate under phosphate starvation and contain larger acidocalcisomes that have increased P_i content. Heterologous expression of *TbPHO91* in *Xenopus* oocytes followed by two-electrode voltage clamp recordings disclosed that *myo*-inositol polyphosphates stimulate both sodium-dependent depolarization of the oocyte membrane potential and P_i conductance. Deletion of the SPX domain in TbPho91 abolished this stimulation. Inositol pyrophosphates such as 5-diphosphoinositol pentakisphosphate generated outward currents in Na^+/P_i-loaded giant vacuoles prepared from WT or from *TbPHO91*-expressing *pho91*Δ strains but not from the *pho91*Δ yeast strains or from the *pho91*Δ strains expressing *PHO91* or *TbPHO91* with mutated SPX domains. Our results indicate that TbPho91 and Pho91p are responsible for vacuolar P_i and Na^+ efflux and that *myo*-inositol polyphosphates stimulate the Na^+/P_i symporter activities through their SPX domains.

Acidocalcisomes are acidic calcium stores rich in P_i, PP_i, and polyphosphate (polyP)[3] bound to cations such as calcium, magnesium, and sodium (1). Synthesis and translocation of polyP into acidocalcisomes of trypanosomes and the acidocalcisome-like vacuoles of *Saccharomyces cerevisiae* are mediated via the vacuolar transporter chaperone (VTC) complex, of which Vtc4 is the catalytic subunit (2, 3).

This work was supported by the NIAID, National Institutes of Health Grant AI077538 (to R. D.). The authors declare that they have no conflicts of interest with the contents of this article. The content is solely the responsibility of the authors and does not necessarily represent the official views of the National Institutes of Health.

[1] These authors contributed equally to this work.
[2] To whom correspondence should be addressed. E-mail: rdocampo@uga.edu.

[3] The abbreviations used are: polyP, polyphosphate; VTC, vacuolar transporter chaperone; 5-IP$_7$, 5-diphosphoinositol pentakisphosphate; PCF, procyclic form; PFA, phosphonoformic acid; NMDG, *N*-methyl-D-glucamine; IP$_6$, inositol hexakisphosphate; PP-IP$_4$, 5-diphosphoinositol tetrakisphosphate; FBS, fetal bovine serum.

It has been shown that rapid hydrolysis of acidocalcisome polyP occurs when trypanosomes are exposed to alkalinizing agents (nigericin, NH_4Cl) or hyposmotic stress (4). Vacuolar polyP is also a source of P_i for dNTP synthesis needed for yeast DNA duplication (5) or for biosynthesis of nucleotides and phospholipids needed for cell division (6). However, how P_i produced by hydrolysis of polyP, catalyzed by endo- and exopolyphosphatases (7–11), is released from these vacuolar compartments or how release is regulated is unknown.

P_i is negatively charged, and it needs to be transported into or out of cells or organelles via an active transport process. P_i transporters use either the transmembrane Na^+ (animals, fungi) or H^+ (plants, bacteria) gradients to drive P_i transport into cells (12). P_i transporters also occur in organelles, such as the mitochondrial proton/phosphate symporter (P_i carrier), an inner membrane-embedded protein that translocates P_i from the cytosol into the mitochondrial matrix (13), and Pho91p, which is a yeast low-affinity vacuolar sodium/phosphate (Na^+/P_i) symporter. Pho91p was proposed to export P_i from the vacuolar lumen to the cytosol (14), although this has never been directly demonstrated. In a previous proteomic study of the acidocalcisomes of *Trypanosoma brucei*, we identified a P_i transporter with similarity to Pho91p, localized it to the acidocalcisome by expressing the HA-tagged protein, and suggested that this transporter, TbPho91, could also be involved in returning P_i to the cytosol after polyP hydrolysis (15).

As occurs with Pho91p (14) and the *Trypanosoma cruzi* Pho91 ortholog (TcPho91), which localizes to the contractile vacuole (16), TbPho91 possesses a SPX domain (named after Syg1 and Pho81, in yeast, and XPR1 in humans), and recent work has shown that SPX domains can bind inositol polyphosphates and act as sensor domains (17, 18). A particularly strong binder is 5-diphosphoinositol pentakisphosphate (5-PP-IP$_5$ or 5-IP$_7$), an inositol pyrophosphate. 5-IP$_7$ has five of the *myo*-inositol hydroxyl groups monophosphorylated, whereas the sixth, at the 5-position, contains a diphosphate group (19).

In this work we investigated the function of TbPho91 by deleting its gene and examining the phenotypic changes in cells. We used the two-electrode voltage clamp method to directly measure membrane electric currents stimulated by inositol polyphosphates in *Xenopus* oocytes heterologously expressing *TbPHO91*, with or without its SPX domain. In addition, we patch-clamped giant vacuoles of yeast expressing either WT or

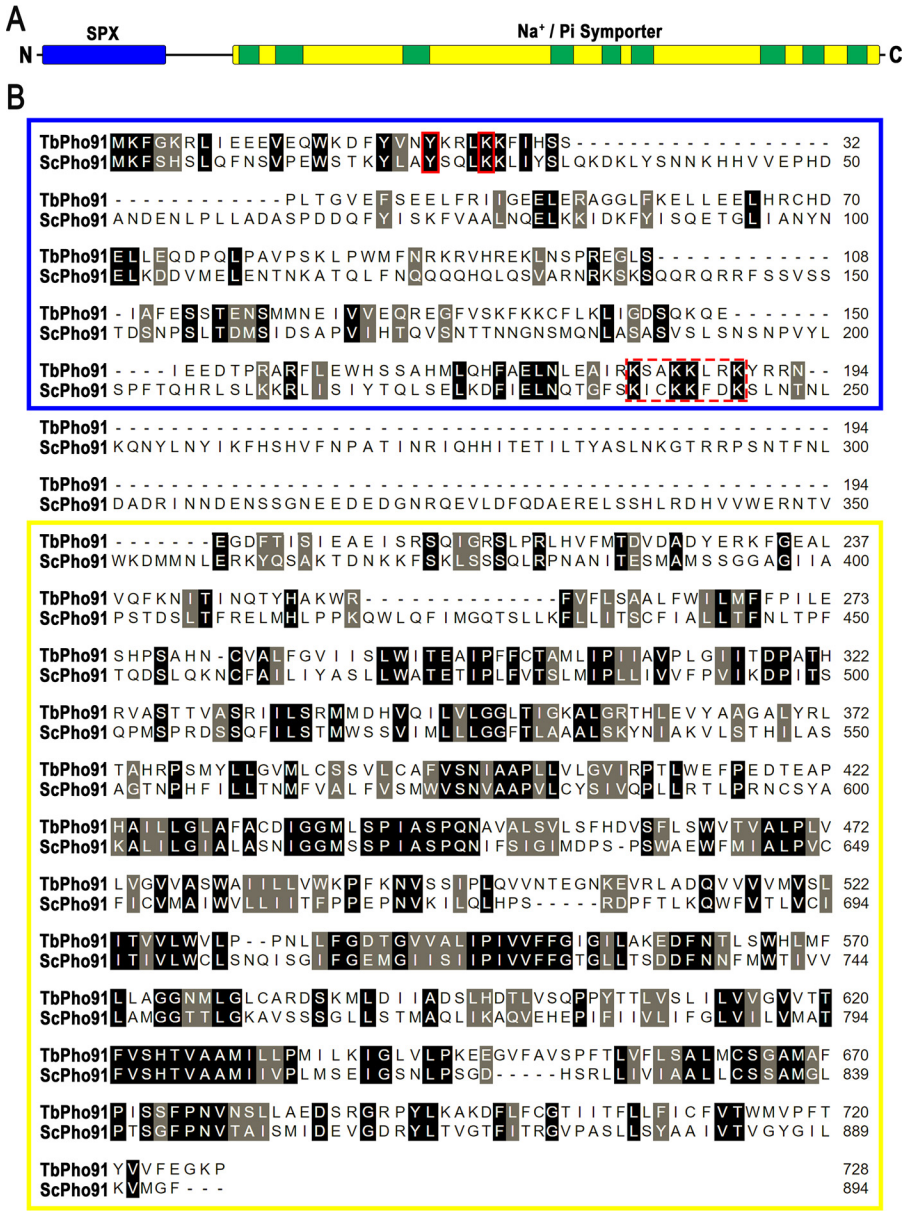

Figure 1. Conserved domains and alignment of TbPho91 and Pho91p orthologs. *A*, conserved domains of TbPho91. The SPX domain (*blue*) has 190, whereas the conserved sodium/sulfate symporter domain (*yellow*) has 472 amino acid residues. There are nine annotated transmembrane domains (*green*). *B*, alignment of amino acid sequence of Pho91s from *T. brucei* and *S. cerevisiae*. Identical (*black*) and similar (*gray*) amino acid residues are *shaded*. Note conservation of canonical residues from the IP_6 phosphate-binding cluster (*solid red boxes*) and the lysine surface cluster (*dashed red box*).

SPX mutant Na^+/P_i symporters. We provide evidence for the role of TbPho91 and Pho91p in P_i and Na^+ release to the cytosol and for their SPX domain-mediated regulation by inositol pyrophosphates.

Results

Characteristics and localization of TbPho91

A gene (Tb427tmp.01.2950), annotated as sodium/sulfate symporter or phosphate transporter and encoding for a putative *PHO91* ortholog, is present in the *T. brucei* genome (http://tritrypdb.org/tritrypdb/)[4] and was named *TbPHO91* (15). The full-length gDNA of *TbPHO91* was cloned by PCR amplification from the Lister 427 strain of *T. brucei,* confirmed by sequencing and shown to be identical to the gene in the database. The orthologs identified in *T. cruzi* (TcCLB.508831.60) and *Leishmania major* (LmjF.28.2930) share 65 and 59% amino acid identity, respectively, to TbPho91. The ORF predicts a 728-amino acid protein with an apparent molecular mass of 81.4 kDa, nine transmembrane domains (Fig. 1*A*), an N-terminal regulatory SPX domain, and an anion-permease domain also present in other anion transporters. In previous work, we reported the endogenous C-terminal tagging of *TbPHO91* with an *HA* tag and the localization of TbPho91-HA predominantly to the acidocalcisomes of *T. brucei* (15). Alignment of Pho91 from *T. brucei* (Protozoa, Euglenozoa) and *S. cerevisiae* (Fungi, Ascomycota) (Fig. 1*B*) shows the conservation of key residues for interaction with inositol polyphosphates in the SPX domain

[4] Please note that the JBC is not responsible for the long-term archiving and maintenance of this site or any other third party hosted site.

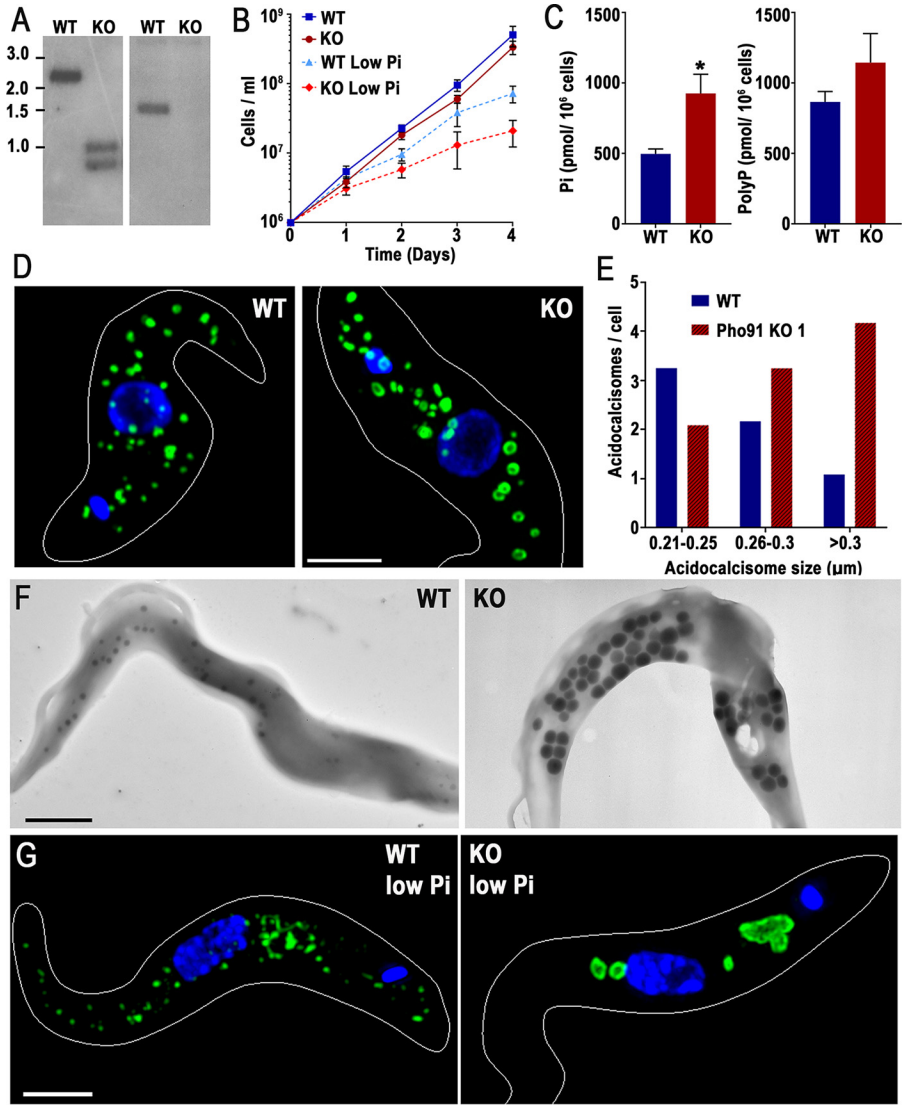

Figure 2. TbPho91 is important for phosphate release from acidocalcisomes. *A*, Southern blot analysis of WT cells and *TbPHO91*-knockout mutants (*KO*). We used two probes to show gene deletion: the use of a 5′-UTR *TbPHO91* probe (*left panel*) shows that the gene was replaced by puromycin- and blasticidin-resistance markers, and the use of a *TbPHO91* probe (*right panel*) shows that the sequence was removed from the genome. *B*, growth curve of WT and *TbPHO91*-KO procyclic forms, under normal or low phosphate (20 μM) medium. *C*, quantification of total P_i and polyP content. The values are means ± S.D., $n = 4$. *, $p < 0.01$. *D*, immunofluorescence microscopy using VP1 antibody to stain acidocalcisomes. *Bar*, 2 μm. *E*, numeric distribution of acidocalcisomes bigger than 0.2 μm by size. Acidocalcisomes from 10 WT and *TbPHO91*-KO cells were counted, in two independent experiments. *F*, transmission EM of representative whole WT cells show acidocalcisomes as electron-dense spheres. *G*, IFA of representative *TbPHO91*-KO cells labeled with VP1 antibody showing larger acidocalcisomes than in WT cells. *Bars*, 1 μm. Acidocalcisomes of *TbPHO91*-KO cells display altered morphology upon phosphate starvation. WT or *TbPHO91*-KO cells were cultured in low phosphate medium (20 μM) for 24 h. WT cells have normal size acidocalcisomes throughout the cell body and a few larger ones between the nucleus and kinetoplast. *TbPHO91*-KO cells displayed a small number of abnormally large acidocalcisomes, with the largest normally observed between the nucleus and kinetoplast. *Bar*, 2 μm.

(17, 18). Moreover, the sodium/sulfate symporter domain is conserved in these organisms (67% similarity and 34% identical residues).

Phenotypic changes in TbPHO91 knockout procyclic forms

We generated knockout mutants of *TbPHO91* in procyclic forms (PCFs) by homologous recombination replacing both copies of the gene with resistance markers and isolated several clones. Southern blot analysis demonstrated that *TbPHO91* was absent in one of these clones (Fig. 2*A*). These *Tbpho91*$^{-/-}$ cells did not show significant growth defect in regular medium but showed a significant growth defect in low phosphate medium (Fig. 2*B*). If TbPho91 is involved in the release of P_i and Na^+ from acidocalcisomes, a possible consequence is the accumulation of P_i (and Na^+) within the organelles with concomitant increase in their osmolarity. This was apparently the case as we detected higher levels of P_i in the mutants with no significant changes in polyP (Fig. 2*C*). Immunofluorescence analysis of *Tbpho91*$^{-/-}$ cells using antibodies against the vacuolar pyrophosphatase (TbVP1), an acidocalcisomal marker, showed enlarged organelles (Fig. 2*D*). The TbVP1 signals appear as small dots in WT cells and as larger ring-like structures in the *Tbpho91* mutants. Mutant cells have increased numbers of larger acidocalcisomes (>0.2 μm) (Fig. 2*E*), and these results were confirmed by direct transmission EM of whole cells. In contrast to WT cells, *Tbpho91*$^{-/-}$ cells contained larger acido-

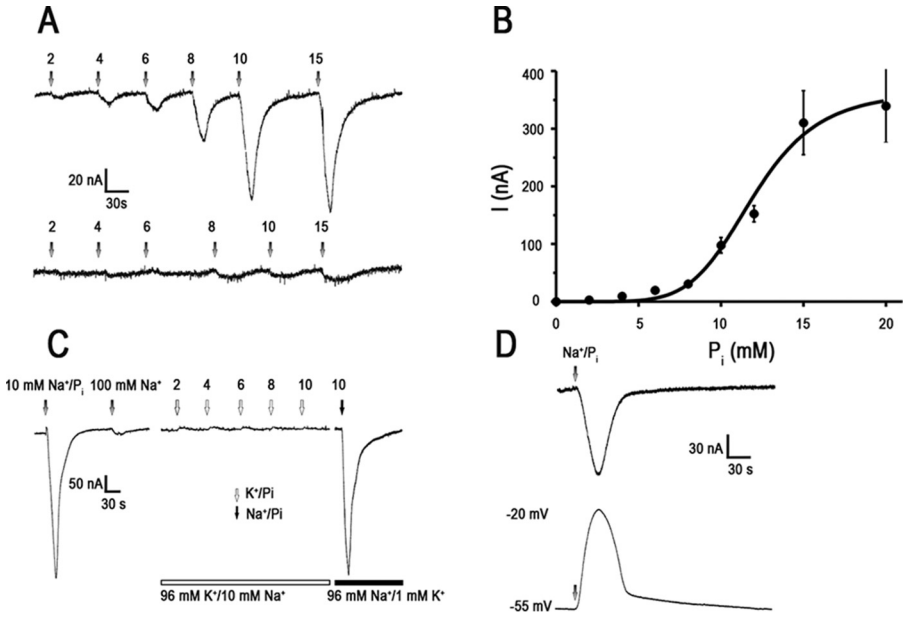

Figure 3. Electrophysiological characterization of TbPho91. *A*, inward currents elicited in the presence of increasing concentrations of Na^+/P_i in *TbPho91*-expressing oocytes (*upper tracing*) or uninjected oocytes (*lower tracing*) (values in mM). *B*, TbPho91 is a low-affinity transporter. Steady-state kinetic parameters were obtained by fitting the peak currents recorded in the presence of increasing concentrations of Na^+/P_i according with the Hill equation. The values are means ± S.E. of three independent experiments. *C*, sodium dependence of TbPho91 activity. No response was detected when Na^+ was used alone or when K^+ was used instead of Na^+ (values in mM). *D*, collapse of V_m in unclamped cells (*lower panel*) when Na^+/P_i is taken up (*upper panel*), indicating membrane depolarization.

calcisomes (Fig. 2*F*). The results are consistent with an increase in the acidocalcisomes osmolarity followed by water accumulation and enlargement. Previous work has shown lower levels of polyP and PP_i when *TcPHO91* was down-regulated (16), but no changes were observed in *pho91*Δ *S. cerevisiae* strains (14). Immunofluorescence microscopy of *Tbpho91*$^{-/-}$ cells grown under P_i starvation conditions showed further dilation of acidocalcisomes, which appeared to fuse in larger vacuoles (Fig. 2*G*). In conclusion our results showing that enlargement of acidocalcisomes increased P_i content and decreased growth rate under P_i starvation stress are consistent with a role for TbPho91 in P_i release from acidocalcisomes.

Functional expression of TbPHO91 in Xenopus laevis oocytes and basic transport characteristics

We investigated the basic transport characteristics of TbPho91 by expressing it in *Xenopus* oocytes. Fig. 3*A* (*upper tracing*) shows the inward currents generated at holding potential (V_h = −60 mV) by addition of different concentrations of Na^+/P_i to oocytes expressing *TbPHO91*. The current amplitude increased in a dose-dependent manner with a threshold around 2 mM, and the results are consistent with transport of a positive charge into the cell. Negligible current changes were observed in control diethylpyrocarbonate-injected oocytes (Fig. 3*A*, *lower tracing*), probably related to endogenous P_i-transporting mechanisms. Fig. 3*B* shows the curve obtained by fitting the peak currents recorded (as measured from the magnitude of the P_i-induced deflection) in the presence of increasing concentrations of P_i. According to the Hill equation, the calculated K_m for P_i was 10.6 ± 1.1 mM (mean ± S.E. of five independent experiments) and shows that TbPho91 is a low-affinity transporter. The addition of 100 mM NaCl alone in the absence of P_i did not result in any significant change in current (Fig. 3*C*, *left*), whereas replacing Na^+ by equimolar concentrations of K^+ did not generate P_i-induced changes in currents (Fig. 3*C*, *right*), demonstrating the sodium selectivity of TbPho91. There was collapse of V_m in unclamped cells, indicating depolarization (Fig. 3*D*, *lower panel*).

Phosphonoformic acid (PFA) is a highly specific competitive inhibitor (20) of solute carrier SLC34 transporters (also called type II Na^+/P_i co-transporters) (12). Treatment of *TbPHO91*-expressing oocytes with 10 mM PFA for 10 min did not impact the amplitude of the Na^+/P_i current (288.3 ± 11.7 nA before PFA and 302 ± 39.3 nA after PFA, n = 4) (Fig. 4*A*), suggesting that TbPho91 could belong to the solute carrier family SLC20 of transporters (also called type III Na^+/P_i co-transporters). The delayed decay of the Na^+/P_i transient observed in Fig. 4*A* was caused by a PFA-induced slow inward current (Fig. 4*B*).

To analyze the voltage dependence of the transporter, we registered the currents generated in oocytes expressing *TbPHO91* in response to a step change in V_h from −80 to +40 mV (Fig. 5*A*). The current amplitude was measured at the steady-state part of the traces. Fig. 5*A* (*left panel*) shows representative raw currents in response to the voltage step protocol when perfused in the absence (−P_i) or presence (+P_i) of 10 mM P_i or after replacing NaCl by *N*-methyl-D-glucamine (NMDG). Quantification of averaged currents of oocytes expressing *TbPHO91* (Fig. 5*A*, *right panel*) shows a significant increase in the steady-state current at positive (280% at +40 mV) and negative (294% at −80 mV) potential in the presence of 10 mM P_i (*red triangles*) when comparing to control conditions without P_i (*black circles*). Sodium dependence is demonstrated by the lack of response when NaCl is replaced by the nonpermeable cation NMDG (*blue line*). These results demonstrate that both Na^+ and P_i are essential for TbPho91 activation. P_i induced a

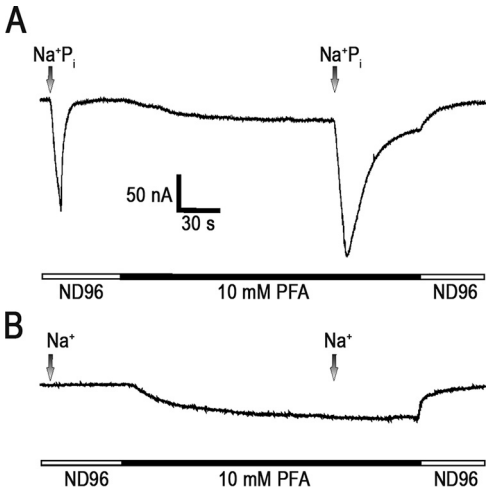

Figure 4. Lack of current inhibition by phosphonoformic acid. *A*, inward current recorded in response to addition of 10 mM Na^+/P_i in ND96 solution. Lack of inhibition of Na^+/P_i-generated inward current upon addition of 10 mM PFA. *B*, there was no significant effect when 10 mM NaCl alone was added.

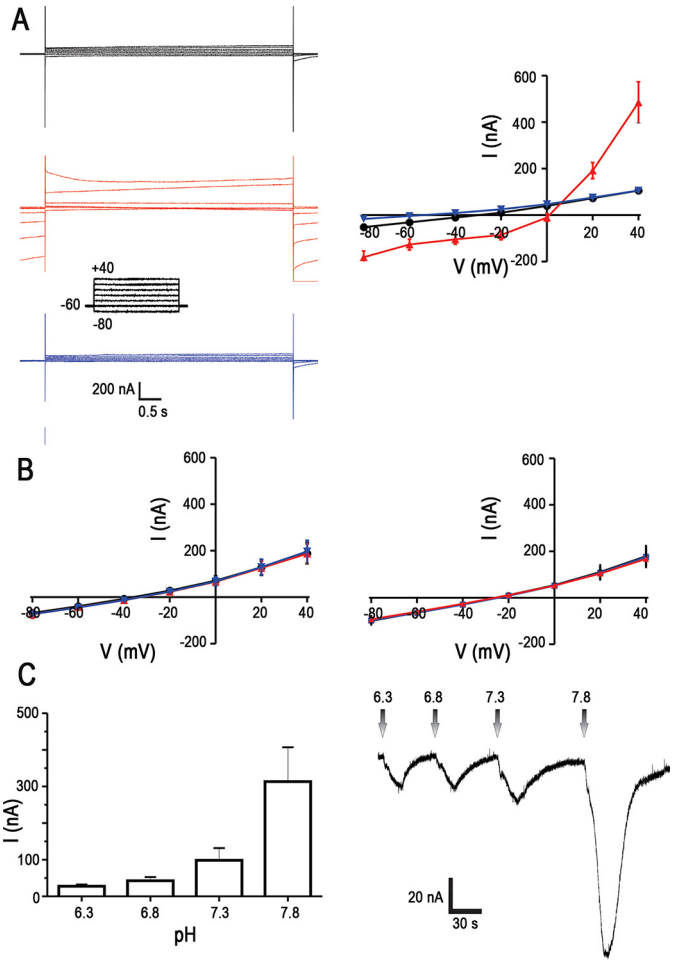

Figure 5. Sodium, anion, and pH dependence of TbPho91. *A*, representative currents recorded in response to a voltage step protocol between −80 and +40 mV in oocytes expressing *TbPho91* when superfused in ND96 solution in the absence (*upper panel*, *black*) or presence (*center panel*, *red*) of 10 mM Na^+/P_i, or substituting NaCl by NMDG (*lower panel*, *blue*). *Right panel*, *I/V* curve of the normalized currents obtained from the voltage protocols showed in *A* in the absence (*black line*) or presence (*red line*) of 10 mM Na^+/P_i or substituting NaCl by NMDG (*blue line*). The values are means ± S.E. ($n = 3$). *B*, anion selectivity analysis of the currents recorded under a voltage step protocol in the presence of sulfate (*left panel*, *red line*) or nitrate (*right panel*, *red line*). The values are means ± S.E. of three independent experiments. *Black lines* are controls without anions. *C*, currents recorded in response to Na^+/P_i addition at different pH levels ($n = 4$) (*left panel*). The values are means ± S.E. of three independent experiments. The *right panel* is from a representative experiment.

430% higher steady-state current at +40 mV than at −40 mV ($p < 0.05$, Student's *t* test, $n = 5$), indicating an outward-rectifying behavior with respect to V_h. Fig. 5*B* shows the anion selectivity by applying voltage pulses in the presence of either 10 mM sulfate (*blue inverted triangles*) or 10 mM nitrate (*blue squares*). No significant changes in the recorded currents were observed when compared with the controls in absence of anions.

The Na^+/P_i current showed strong dependence on the pH of the extracellular medium (Fig. 5*C*, *left panel*). Fig. 5*C* (*right panel*) shows a representative recording of currents, at different pH levels, in the presence of 10 mM P_i. The current amplitude in presence of 10 mM P_i was increased by 318%, from 98.9 ± 33.6 nA at pH 7.3 to 313.7 ± 93.7 nA at pH 7.8 (*, $p < 0.05$, $n = 6$). On the other hand, the shift of extracellular pH to more acidic values produced a decrease by 232% in the current amplitude to 42.7 ± 10.1 nA at pH 6.8 (*, $p < 0.05$, $n = 6$) or by 359% to 27.5 ± 4.8 nA (**, $p < 0.05$, $n = 6$) at pH 6.3 (Fig. 5*C*, *right panel*), which is more typical for type II than for type III Na^+/P_i co-transporters (21).

Complete removal of extracellular calcium from the bath solution (100 μM EGTA added) tended to amplify the Na^+/P_i current, a change that, however, was not significant ($p < 0.2$, $n = 5$) (Fig. 6). Extracellular calcium concentrations above 1.8 mM were not tested, because this induced rapid death of oocytes. Taking into account its electrogenicity, low P_i affinity and resistance to PFA treatment, we suggest that TbPho91 belongs to the type III Na^+/P_i co-transporters family (SLC20) (21), although in contrast to other SLC20 proteins (22, 23), Na^+/P_i currents were decreased at lower pH levels.

Modulation by inositol pyrophosphates of the Na^+/P_i conductance of TbPho91 is SPX-dependent

It has been demonstrated that the SPX domains present in the N-terminal of phosphate transporters, VTCs, and signaling proteins act as inositol polyphosphate sensor domains by binding inositol polyphosphates and stimulating polyphosphate synthesis by VTCs in yeast (17). Although different SPX domains bind inositol hexakisphosphate (IP_6) and inositol pyrophosphates like 5-IP_7 with similar affinities *in vitro*, it has been suggested that diphosphoinositol phosphates may be the relevant signaling molecules *in vivo* (17). We therefore investigated whether this was also the case with TbPho91. Preincubation of oocytes for 5–6 min with $InsP_6$, in the μM range (Fig. 7, *A* and *B*) or with 5-IP_7 (Fig. 8*A*) or 5-diphosphoinositol tetrakisphosphate (PP-IP_4) (Fig. 8*B*) in the nanomolar range induced slow inward currents with subsequent amplification of the Na^+/P_i–transmembrane current evoked by 10 mM P_i. The threshold for statistically significant amplification of the Na^+/P_i current was 100 μM for IP_6 (+82.5 ± 39.5%; *, $p < 0.05$, $n = 4$) (Fig. 7*C*). For 5-IP_7, the amplification threshold was 50 nM (+9.2 ± 3.5%; *, $p < 0.05$, $n = 5$), and for PP-IP_4, it was 1 μM (+61.7 ± 26.6%; *, $p < 0.05$, $n = 4$) (Fig. 8*C*). Further increases

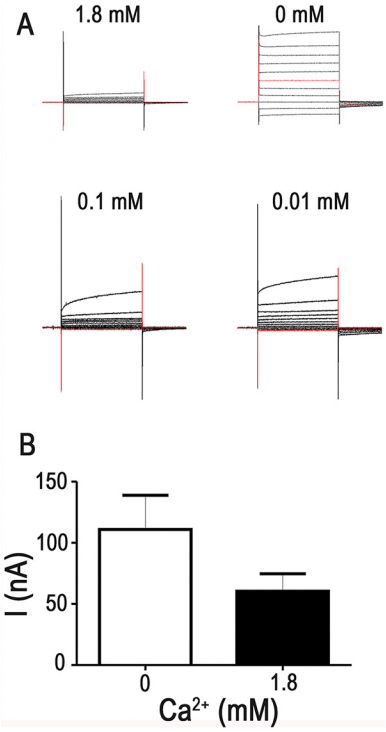

Figure 6. Effect of calcium on TbPho91 currents. *A*, currents elicited by Na^+/P_i in the absence or presence of different concentrations of $CaCl_2$. *B*, currents in the absence or presence of 1.8 mM $CaCl_2$. The values are means ± S.E. of three independent experiments ($p < 0.05$).

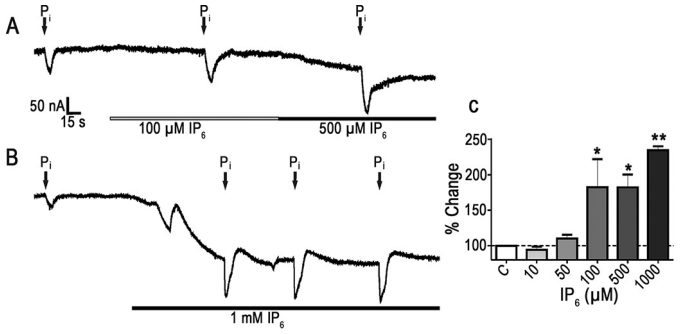

Figure 7. Effect of IP_6 on P_i-elicited currents in oocytes expressing TbPho91. *A*, representative currents recorded when addition of Na^+/P_i was done in the absence or presence of 100 and 500 μM (*upper panel*) or 1 mM (*lower panel*) IP_6. *B*, effect of different concentrations of IP_6 on currents elicited by Na^+/P_i. The values are means ± S.E. of three independent experiments. *C*, *, $p < 0.05$; **, $p < 0.01$, as compared with control (*lane C*) without IP_6.

of the phosphate-containing ligands enhanced the amplification of the Na^+/P_i currents (Figs. 7*C* and 8*C*).

To investigate whether the phosphate-containing ligands were acting through the SPX domain of TbPho91, we expressed the protein with a deletion of this domain (TbPho91-ΔSPX) and examined its response to 5-IP_7 and PP-IP_4. Neither 5-IP_7 nor PP-IP_4 (Fig. 8, *A* and *B*) could amplify the currents induced by 10 mM P_i addition in *TbPHO91-ΔSPX*-expressing oocytes.

SPX-dependent Na^+/P_i release from yeast vacuoles

Acidocalcisomes have a diameter of ~200 nm, and it is very difficult to do patch-clamp studies with these small organelles to test Na^+/P_i currents. Because the yeast vacuole has many similarities to the trypanosome acidocalcisome, we used giant

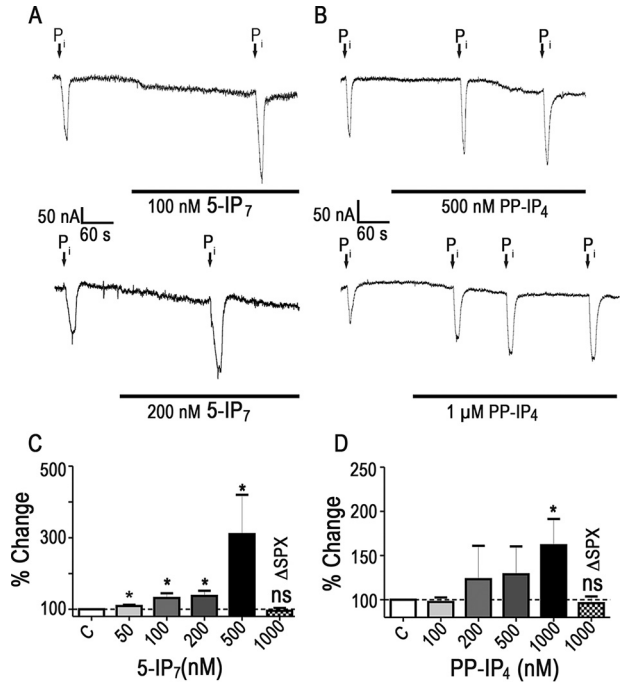

Figure 8. Effect of 5-IP_7 and PP-IP_4 on P_i-elicited currents in oocytes expressing TbPho91 and ΔSPX-TbPho91. *A*, representative currents recorded when addition of Na^+/P_i was done in the absence or presence of 100 nM (*upper panel*) or 200 nM (*lower panel*) 5-IP_7. *B*, representative currents recorded when addition of Na^+/P_i was done in the absence or presence of 500 nM (*upper panel*) or 1 μM (*lower panel*) PP-IP_4. *C* and *D*, effect of different concentrations of 5-IP_7 (*C*) or PP-IP_4 (*D*) on currents elicited by Na^+/P_i. The values are means ± S.E. of three independent experiments. *, $p < 0.05$, as compared with control (*lanes C*) without inositol pyrophosphates. ΔSPX are oocytes expressing truncated TbPho91 without the SPX domain.

vacuoles (up to ~20 μm in diameter) from yeast instead. This method has the additional advantage over the *Xenopus* studies that it is possible to eliminate endogenous currents by inactivation of the genes in yeasts. We prepared giant cells of *S. cerevisiae* by the spheroplast incubation method using 2-deoxy-glucose to inhibit cell wall synthesis (24). When using this method and when the giant cells are treated by moderate hyposmotic shock, only the plasma membranes are disrupted, and giant vacuoles are released. It is then possible to attach a patch pipette to isolated vacuoles and rupture the patch membrane using a high voltage pulse (Fig. 9*A*). The vacuolar lumen, which is connected to the pipette (whole-vacuole configuration), can then be loaded with a solution containing Na^+ and P_i to monitor the currents across the membrane. We generated a knockout of *PHO91* using homologous recombination to replace the genomic sequence of *PHO91* by a resistance marker and used these cells to express mutant or WT *PHO91* and *TbPHO91*. A previous high-throughput screening assay reported *pho91*Δ mutants as having a small defect in vacuolar fragmentation (25). However, we did not find morphological alterations in the vacuoles of *pho91*Δ (data not shown).

Once vacuoles were released by hyposmotic shock of giant cells, they were patched and clamped at a voltage of +60 mV. The bath solution had 10 mM Hepes, pH 7.1, containing 100 mM NaCl, 200 mM sorbitol, and 1 mM $MgCl_2$, whereas the pipette solution contained the same mixture plus 10 mM $NaHPO_4$-Na_2HPO_4 to detect outward currents generated by displace-

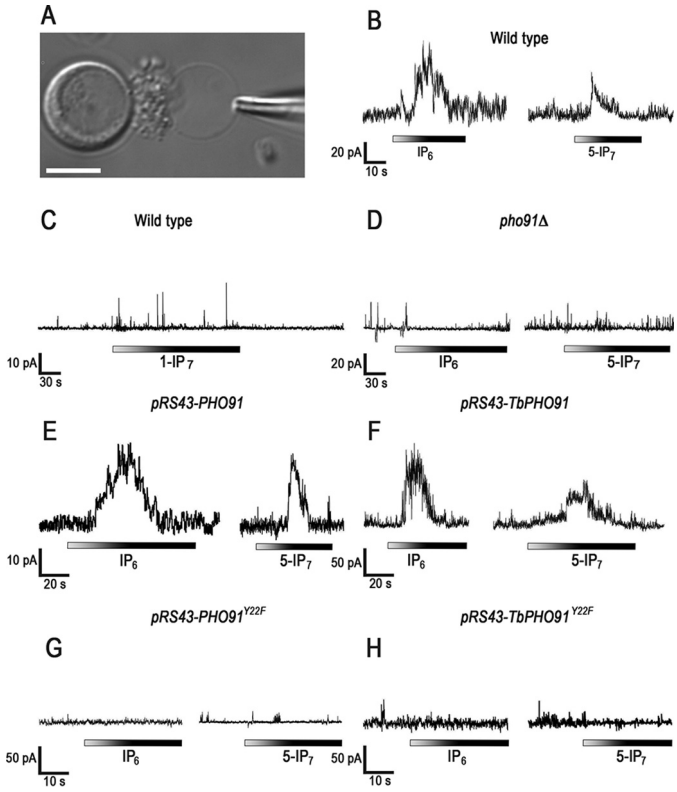

Figure 9. IP_6 and 5-IP_7 induce SPX domain-mediated activation of Na^+/P_i currents in *PHO91*- and *TbPho91*-expressing vacuoles. *A*, image shows a intact giant cell of *S. cerevisiae* and a vacuole isolated after hyposmotic shock showing a patch pipette attached to it. *Bar*, 10 μm. *B*, activation of Na^+/P_i outward currents in vacuoles from WT yeast after injection of IP_6 (1 mM) or 5-IP_7 (1 μM). *C*, effect of 1 μM 1-IP_7 on WT yeast vacuoles. *D*, *pho91*Δ vacuoles do not produce currents after application of IP_6 or 5-IP_7. *E* and *F*, complementation of *pho91*Δ with *PHO91* (*E*) or *TbPHO91* (*F*) restores vacuole response to IP_6 and 5-IP_7. *G* and *H*, complementation of *pho91*Δ with mutated $PHO91^{Y22F}$ (*G*) or $TbPHO91^{Y22F}$ (*H*) does not restore vacuole ability to generate Na^+/P_i currents. The data are representative of two to four independent experiments.

ment of Na^+/P_i from the vacuoles to the bath solution ("cytosol"). Application of 1 mM IP_6 or 1 μM 5-IP_7 to the bath solution (Fig. 9*B*) induced outward currents of 169.3 ± 28.1 and 102 ± 22.5 pA (n = 4), whereas no significant currents were detected when 1-IP_7 (the other IP_7 present in yeast (18)) was used (Fig. 9*C*) or when IP_6 or 5-IP_7 was applied to vacuoles from *pho91*Δ cells (Fig. 9*D*).

Next we generated plasmid constructs for expression of *PHO91* or *TbPHO91* in *pho91*Δ cells. We cloned the genomic sequence of *PHO91* or *TbPHO91* in plasmid vector pRS413 that maintains a single copy per cell, and to ensure expression at endogenous levels, we also inserted the upstream promoter region of *PHO91*. We then compared the response of giant vacuoles from *PHO91*Δ complemented with exogenous *PHO91* (22.2 ± 0.75 and 29.6 ± 3.6 pA for IP_6 and IP_7, respectively, n = 2) or *TbPHO91* (46.5 ± 8.3 and 26.3 ± 2.5 pA for IP_6 and IP_7, respectively, n = 4) genes (Fig. 9, *E* and *F*) or with exogenous *PHO91* and *TbPHO91* genes mutated in the tyrosines (Tyr^{22}) of the phosphate-binding cluster of the SPX domains (Fig. 9, *G* and *H*) described previously as important for binding to inositol polyphosphates (18). Complementation using constructs that express $PHO91^{Y22F}$ or $TbPHO91^{Y22F}$ resulted in significantly reduced or completely abolished currents induced by IP_6 or 5-IP_7 (Fig. 9, *G* and *H*). Taken together, our results show that inositol polyphosphates trigger the release of Na^+/P_i by Pho91 symporters in an SPX-dependent manner.

Discussion

We report the biochemical and electrophysiological characterization of a Na^+/P_i symporter of *T. brucei*. This transporter, which is an ortholog to *S. cerevisiae* Pho91p, localizes to the acidocalcisomes and is essential for normal growth of PCF trypanosomes in P_i starvation medium. These conditions can be expected when PCF are in the intestine of the tsetse flies under starvation conditions (26) but not in the bloodstream forms (BSF) that are in contact with P_i concentrations in the 1–1.4 mM range (27). The results suggest a role for P_i produced by hydrolysis of acidocalcisome polyP in cell division under P_i starvation conditions, as occurs in yeast (6). Functional expression in *X. laevis* oocytes followed by two-electrode voltage clamp recordings showed that TbPho91 is a low-affinity, sodium-dependent, and P_i-selective transporter. Application of nanomolar concentrations of 5-IP_7, resulted in Na^+-dependent depolarization of the oocyte membrane potential and increase in the P_i conductance. Deletion of the SPX domain abolished the stimulation produced by 5-IP_7. Expression of TbPho91 or Pho91p in giant vacuoles of *pho91*Δ cells allowed the determination of their role in Na^+/P_i release and their SPX-dependent regulation by inositol polyphosphates.

TbPHO91-KO PCF trypanosomes had a normal growth rate in rich medium but decreased growth in P_i starvation medium. These cells did not have significant differences in the levels of polyP. This last result is in agreement with results obtained with *pho91*Δ strains that showed (as *TbPHO91*-KO cells) a slight but not significant increase in polyP (14). The results suggest that polyP levels of *T. brucei* and *S. cerevisiae* vacuoles are mainly controlled through synthesis and not through degradation and release and are in agreement with results where overexpression of the regulatory subunit of the VTC complex leads to higher polyP levels in yeast (28). The results are also consistent with the model proposed in yeast, where polyP serves as a buffer that can be mobilized during phosphate limitation to temporarily maintain internal P_i levels (29). In contrast, the *T. cruzi* ortholog (TcPho91) localizes to the contractile vacuole of the parasite, and down-regulation of its expression reduces the levels of short chain polyP and PP_i (16), suggesting that release of P_i is regulating PP_i and polyP levels in this organelle. Overexpression of TcPho91 results in transfer of the protein to the plasma membrane and higher levels of PP_i and short-chain polyP consistent with an enhanced P_i transport (16).

Acidocalcisomes of *TbPHO91*-KO PCF appear to fuse with each other under P_i starvation, resulting in enlarged vacuoles. This phenotype suggests homotypic fusion. In this regard, it has been reported that a VAMP7 ortholog present in acidocalcisomes of *T. cruzi* has a role in their fusion to the contractile vacuole under hyposmotic stress (30).

Experiments in *Xenopus* oocytes allowed the characterization of TbPho91 and revealed its SPX-dependent activation by IP_6 and 5-IP_7. One of the drawbacks of using these cells is the difficulty of making deletion mutants. This is essential to suppress endogenous currents that could interfere with currents

Table 1

Primers used in this study

For the last five primers, T_7 promoter or polyT_{30} sequences are underlined. Kozak consensus sequences for increasing efficiency of translation initiation are in bold. Gene-specific sequences are italicized. Additional nucleotides upstream of the T_7 promoter or the Kozak consensus sequence are incorporated into the primers for desirable *in vitro* transcription/translation in *Xenopus laevis* oocytes.

Primer	Use
CATGCATATTGACTTTAGGTCCTCTTGGTACCTTTCCCTCTGCTCTTCCTGTTCCCTTCTTATTTTTAGTCCCGACAGTGCAGGCACGCCACTGCCGCATAAACTACGGT	Knockout *TbPHO91*; used to amplify resistance markers from pPOTv6 plasmids
ATAATAACAATAATGACAGCACGACGAAACCGCAGTCCAGCTCCTGTACCCTTCTGTCGATGCGAACGGAACAAGACAACGCCAACTAAATGGGCACTCG	Knockout *TbPHO91*; used to amplify resistance markers from pPOTv6 plasmids
GCGAAGTGGCGTTTTGTCTT	Southern blot probe for coding sequence of *TbPHO91*
AGACGCTGCTACACAGCATT	Southern blot probe for coding sequence of *TbPHO91*
TAGCGGTGCAGCTCTAGTTC	Southern blot probe for 5′-UTR sequence of *TbPHO91*
GGGAAAGGTACCAAGAGGACC	Southern blot probe for 5′-UTR sequence of *TbPHO91*
AGGAAAAATGCCGCTCAAAATCT	Knockout of yeast *PHO91*
CAATACAAATGGGCATTGACCAGA	Knockout of yeast *PHO91*
TTGGGTACCGGGCCCCCCCTCGAGGTGGGCCTATCCGCCTTAAT	Amplification of *PHO91* for cloning in pRS413
GGATCCCCCGGGCTGCAGGAATTCAATCATAAGTGGTGCGGCCA	Amplification of *PHO91* for cloning in pRS413
GACACGGTAACTTGCAGACTGACATGAAGTTCGGAAAGCG	Amplification of *TbPHO91* for fusing with *PHO91* UTRs and clone in pRS413
TTTCATTCTCTCTATGGATAATCCTACGGTTTGCCTTCAAA	Amplification of *TbPHO91* for fusing with *PHO91* UTRs and clone in pRS413
TTGGGTACCGGGCCCCCCCTCGAGGTGGGCCTATCCGCCTTAAT	Amplification of *PHO91* 5′-UTR for fusing with *TbPHO91*
GTCAGTCTGCAAGTTACCGTGTCACCTTCACAGTTTTCTTTTTATTTG	Amplification of *PHO91* 5′-UTR for fusing with *TbPHO91*
GATTATCCATAGAGAGAATGAAAGGTTACTAATATAGTATGTATACGTGC	Amplification of *PHO91* 3′-UTR for fusing with *TbPHO91*
GGATCCCCCGGGCTGCAGGAATTCAATCATAAGTGGTGCGGCCA	Amplification of *PHO91* 3′-UTR for fusing with *TbPHO91*
GCTGCGAAAAGGCCAGATACTTGG	Amplification of *PHO91* fragment with Y22F mutation
CCAAGTATCTGGCCTTTTCGCAGC	Amplification of *PHO91* fragment with Y22F mutation
TATGTAAATTTCAAACGGCTGAAAAAGTTCATACACAGTTCC	Amplification of *TbPHO91* fragment with Y22F mutation
GCCGTTTGAAATTTACATAGAAATCTTTCCACTGCTCCA	Amplification of *TbPHO91* fragment with Y22F mutation
CCCGCGAAATTAATACGACTCACTATAGGGAGA**CCACC***ATGAAGTTCGGAAAGCGGC*	*TbPHO91T7F* (for *Xenopus* expression)
CCCGCGAAATTAATACGACTCACTATAGGGAGA**CCACC***ATGGAAGCAGAGATTAGCCG*	*TbPHO91TFN* (for *Xenopus* expression)
TTTTTTTTTTTTTTTTTTTTTTTTTTTTTTTT*CTACGGTTTGCCTTCAAACAC*	*TbPHO91T30R* (for *Xenopus* expression)
CCCGCGAAATTAATACGACTCACTATAGGGAGA**CCACC***ATGAAGTTCTCGCATTCCT*	*PHO91T7F* (for *Xenopus* expression)
TTTTTTTTTTTTTTTTTTTTTTTTTTTTTTTT*CTAAAATCCCATTACTTTCAATATGCC*	*PHO91T30R* (for *Xenopus* expression)

caused by the transporter under investigation (24). This problem sometimes is solved by overexpression of the exogenous transporter, but a more adequate solution is to use giant vacuoles of *S. cerevisiae* that have been deprived of the endogenous transporter (24). An additional advantage of this system is that once patched, vacuoles could be loaded with Na^+/P_i, and the currents detected indicate their release to the cytosolic site. Using this technique we directly demonstrate for the first time that Pho91 and TbPho91 release Na^+/P_i to the cytosolic site of the vacuoles. 5-IP7 directly stimulates this activity.

Until now inositol pyrophosphates have been shown to stimulate only one SPX domain–controlled process: polyP synthesis by the VTC complex of isolated yeast vacuoles. Both 1-IP_7 and 5-IP_7 (the two isomers that have been found in living cells) stimulate polyP synthesis with an EC_{50} of 300–500 nM. However, our results showed that under similar conditions 5-IP_7, but not 1-IP_7, was able to generate currents in giant vacuoles harboring either TbPho91 or Pho91p. This differential stimulatory activity of these physiological isomers could be important, at least in yeast, to explain the paradoxical simultaneous SPX-dependent stimulation of a polyP synthesis and P_i release from the same vacuoles. It is also possible that other post-translational modifications are involved in the differential stimulation of the two mechanisms.

In conclusion, we have characterized a Na^+/P_i symporter of *T. brucei* and revealed that inositol pyrophosphates stimulate its activity and that of its yeast ortholog, through their SPX domains. The symporters were shown to be involved in the release of P_i and Na^+ to the cytosolic side of the vacuoles, and the results expand the signaling functions of inositol pyrophosphates in regulating P_i metabolism.

Experimental procedures

Chemicals and reagents

Phusion high-fidelity DNA polymerase and the Gibson Assembly® cloning kit were from New England Biolabs (Ipswich, MA). Guinea pig polyclonal antibody against TbVP1 was described previously (31). Alexa-conjugated secondary antibodies were purchased from Invitrogen (Thermo Fisher Scientific). The primers were purchased from Integrated DNA Technologies (Coralville, IA). All other reagents of analytical grade were purchased from Sigma–Aldrich. 5-IP_7, 1-IP_7, and PP-IP_4 were synthesized as described previously (17).

Cell cultures

T. brucei Lister 427 strain PCF were cultivated at 28 °C in SDM-79 medium (32) supplemented with 10% heat-inactivated fetal bovine serum and hemin (7.5 mg/ml). For growth in low phosphate medium, the cells were grown in SM medium (32) produced without phosphate and supplemented with heat-inactivated fetal bovine serum (FBS). FBS phosphate content was measured using the Malachite Green assay. Addition of 1% or 5% FBS resulted in a final P_i concentration of 20 or 100 μM P_i, respectively.

Yeast strains

We used *S. cerevisiae* strain BY4741 (*MATa his3Δ1 leu2Δ0 met15Δ0 ura3Δ0*). To generate *pho91*Δ, we amplified the sequence of KanMX4 resistance marker containing homology to the 100 nucleotides upstream and downstream of *PHO91* coding sequence using the primers listed in Table 1. BY4741 was transformed with the resulting amplicon via the standard lithium acetate technique (33) and selected for growth on YPD plates supplemented with G418. Constructs for yeast comple-

mentation were built on plasmid pRS413 using a Gibson Assembly® cloning kit following the manufacturer's recommendations. To generate inserts, we amplified by PCR the genomic region of *PHO91* gene, including 400 bp upstream and downstream of coding sequence, using primers listed in Table 1. *TbPHO91* insert was built by two-step PCR in which we first amplified the genomic sequence of *TbPHO91* and UTR genomic sequences of *PHO91* using primers with homologous 5′ sequences. Then we used the previous PCR products as template to generate a new single PCR product with Phusion high-fidelity DNA polymerase.

Preparation and isolation of giant yeast vacuoles

Preparation of giant yeast from WT and *pho91*Δ mutants was done as described previously (24) with some modifications. Briefly, mid-log phase yeast were centrifuged; resuspended in 0.1 M Tris-HCl, pH 7.2, and 5 mM DTT; and incubated on a shaker at 50 strokes/min for 10 min. The cells were centrifuged again, washed once with distilled water supplemented with 1 mM DTT, and resuspended in 0.1 M Tris-HCl, pH 7.2, 1 mM DTT, 1 M sorbitol, and 1 mg/ml Zymolyase. The cells were incubated on the shaker for 30 min at room temperature. Once the cells were confirmed to fully convert to spheroplasts, they were centrifuged, and the pellet was carefully resuspended in 6 ml of YPD medium supplemented with 1 M sorbitol and 0.05% 2-deoxy-D-glucose. The cells were then incubated at 25 °C overnight on a shaker at 50 strokes/min. Giant vacuoles were prepared from giant spheroplasts by hyposmotic shock in the recording chamber of the patch-clamp apparatus by incubating the spheroplasts in 10 mM Hepes, pH 7.1, containing 100 mM KCl, 100 mM sorbitol, and 1 mM $MgCl_2$. Then we raised osmolarity to prevent disruption of vacuoles by keeping them in 10 mM Hepes, pH 7.1, containing 100 mM NaCl, 200 mM sorbitol, and 1 mM $MgCl_2$. Patch-clamp recordings were performed on vacuoles attached to the poly-L-lysine–coated chamber. Solution inside the micropipette was 10 mM Hepes, pH 7.1, containing 100 mM NaCl, 200 mM sorbitol, 1 mM $MgCl_2$, 5 mM NaH_2PO_4, and 5 mM Na_2HPO_4, whereas bath solution was the same without the addition of NaH_2PO_4 and Na_2HPO_4.

Sequence analysis

The analysis of TbPho91 sequence (gene ID Tb427tmp.01.2950) was performed using Geneious® 10.2.3 software for alignments and BLASTp for searching homologous sequences Information on number of transmembrane domains and other general information available for this sequence was obtained from TriTrypDB (34).

Molecular constructs for TbPho91 mutant cell lines

For *TbPHO91* knockout construction in PCF, one *TbPHO91* allele was knocked out by replacement with a puromycin selectable marker. This cassette was obtained by PCR using primers shown in Table 1 containing 100–120 nucleotides from the 5′- and 3′-UTRs flanking regions of the *TbPHO91* ORF and the pPOTv6 vector (35) as template. The second allele was knocked out using the same strategy by replacement with a blasticidin selectable marker. The linear constructs were used for transfection of PCF and selection of stable resistant clones. Cell transfections were done as described previously (2). Following each transfection, resistant cells were selected and cloned by limiting dilution in SDM-79 medium containing 10% FBS with appropriate antibiotics (1 μg/ml puromycin, 5 μg/ml blasticidin S) in 24-well plates. Integration of the constructs into genomic DNA of each transfectant was verified by PCR and Southern blot analysis.

Southern blot analysis

This was done as described previously (2). Briefly, we extracted genomic DNA from *T. brucei* and digested 3 μg of DNA with EcoRI and NdeI (probe for 5′-UTR) or HindIII and NotI (probe for coding sequence). Digestion products were resolved by electrophoresis in 0.8% agarose gels, and the DNA was transferred to Zeta-probe blotting membranes (Bio-Rad) by capillarity using 400 mM NaOH. The membranes were hybridized with a radiolabeled *TbPHO91* probe, generated by PCR using primers listed in Table 1 to generate probes for the 5′-UTR and coding sequence of the gene, and labeled with [α-^{32}P]dCTP using random hexanucleotide primers and the Klenow fragment of DNA polymerase I (Prime-a-Gene labeling system; Promega). The membranes were analyzed with a PhosphorImager.

Fluorescence and EM

Immunofluorescence assays with *T. brucei* PCF trypanosomes were done as described previously (2). Antibodies against TbVP1 were used at a dilution of 1:100. Imaging of whole *T. brucei* PCF and determination of morphometric parameters were done as described previously (36).

P_i and polyP quantification

10^6 cells/ml were washed twice in buffer A with glucose (116 mM NaCl, 5.4 mM KCl, 0.8 mM $MgSO_4$, 50 mM Hepes, pH 7.3, and 5.5 mM glucose) and immediately resuspended in 100 μl of ice-cold 0.5 M perchloric acid. Lysate was incubated on ice for 5 min and centrifuged at 15,000 × *g* for 5 min at 4 °C to remove cell debris. The supernatant was transferred to a new tube, and the pH neutralized with 0.8 M KOH, 0.8 M $KHCO_3$. Precipitated $KClO_4$ was removed by centrifugation at 15,000 × *g* for 5 min, and the supernatant was transferred to a new tube. The final volume of the solution was adjusted to 200 μl. One-half was used for phosphate quantification, and the other half was used for polyP determination. P_i and polyP levels were determined using the Malachite Green assay (37) with some modifications. In case of polyP, the levels were determined from the amount of P_i released upon treatment with an excess of recombinant *S. cerevisiae* exopolyphosphatase. PolyP extracts were incubated for 1 h at 37 °C with 50 mM Tris-HCl, pH 7.4, 2.5 mM $MgSO_4$, and 3000–5000 units of purified yeast rPPX. One unit corresponds to the release of 1 pmol of P_i/min at 37 °C. Malachite Green reagent mix was prepared at least 10 min before use, by mixing 0.045% Malachite Green in water with 4.2% ammonium molybdate in 4 M HCl at a 1:3 ratio, respectively, and the solution was filtered with syringe filter units (Millipore). After mixing samples with reagent, we immediately read absorbance at A_{660}. Absorbance values that were within the standard curve done with dilutions of 250 μM KH_2PO_4 were

adjusted for a dilution factor and used to determine final P_i or polyP concentration.

Preparation and maintenance of oocytes

X. laevis oocytes were purchased from Xenoocyte™ (Dexter, MI) and used as standard heterologous expression system for the study of cloned Na^+/P_i co-transporters. Stage IV–V surgically collected oocytes were manually defolliculated and devitellinized with collagenase (1 mg/ml) for 1 h at room temperature and then maintained in filtered Barth's solution (containing 88 mM NaCl, 1 mM KCl, 0.82 mM $MgSO_4$, 0.41 mM $CaCl_2$, 2.4 mM $NaHCO_3$, 0.33 mM $Ca(NO_3)_2$, 10 mM Hepes, plus 50 μg/ml gentamicin, pH 7.4) at a density of less than 100/60-mm plastic Petri dish. The Barth's solution was replaced daily.

cRNA production

Full-length (Tb427tmp.01.2950), truncated *TbPHO91* (*TbPHO91-ΔSPX*), which was obtained by removal of the 606-nucleotide sequence of *TbPHO91* encoding the N-terminal putative SPX domain (residues 1–202), and *PHO91* (GenBank™ accession number NM_001183190) ORFs were amplified with PrimeSTAR HS DNA polymerase (Clontech) from *T. brucei* or *S. cerevisiae* genomic DNA, respectively, by PCR using the corresponding gene specific primers flanking a T_7 promoter, Kozak consensus sequence, or polyT_{30} sequence as indicated in Table 1. The PCR products were gel-purified using QIAquick gel extraction kit (Qiagen) according to the manufacturer's instructions, and the double-stranded nucleotide sequences were confirmed by sequencing at GENEWIZ (Research Triangle Park, NC). cRNAs were obtained by *in vitro* transcription using the purified PCR products as templates with mMESSAGE mMACHINE kit (Ambion Life Technologies, Thermo Fisher Scientific) according with the manufacturer's protocol and verified by denaturing agarose gel electrophoresis and ethidium bromide staining.

cRNA injection

A horizontal Flaming/Brown micropipette puller P-97 (Sutter Instruments) was used to prepare injection capillary micropipettes of 3–4 MΩ. Tips of micropipettes were then polished with Micro Forge MF-830 (Narishige, Tokyo, Japan) to reach 10–30-μm tip diameter for cRNA injection. Capillary micropipettes were then backfilled with sterile mineral oil and filled with 3–5 μl of cRNA solution. 40 ng of cRNA (41.4–50.6 nl) per oocyte was injected using Nanoject II system (Drummond Scientific) and incubated for at least 72 h at 19 °C. Control oocytes were injected with same amount of diethylpyrocarbonate water.

Electrophysiology

The standard two-electrode voltage-clamp technique was used, as described previously (38). Briefly, oocytes were placed in a small volume (200 μl) perfusion chamber (RC-3Z; Warner Instruments, Hamdem, CT) and superfused with ND96 solution at room temperature. Intracellular recording electrodes made of borosilicate glass capillaries with tip resistance of ~3 MΩ were backfilled with 3 M KCl. For best temporal resolution and minimization of errors KCl–agarose bridges connected with Ag/AgCl ground electrodes were used. Pho91 activities were evaluated by whole cell voltage clamp in an Oocyte Clamp OC-725 amplifier (Warner Instruments). Recordings were filtered at 500 Hz, digitized at 16-bit 5 kHz using a Digidata 1440 (Axon Instruments, Molecular Devices), and analyzed using PClamp 10 software (Axon Instruments). All experiments were performed at −60 mV holding potential. Steady-state currents were recorded in the range from −80 to +40 mV during a 1-s period with repeatable 20-mV steps. Responses to P_i and other anions were always examined at holding potential in the presence or absence of sodium. For I/V curve construction, currents were normalized at −80 mV. Each experiment was done with at least four oocytes from two different frogs. The quality criteria used for evaluation of cells suitable for electrophysiological recording were a resting membrane potential lower than −30 mV, a leak current smaller than 100 pA, and a resting membrane potential at the end of experiment lower or equal to those at its start.

All recordings were obtained at room temperature. The oocytes were bathed in ND96 buffer bath solution (96 mM NaCl, 2 mM KCl, 5 mM $MgSO_4$, 1 mM $CaCl_2$, 2.5 mM Hepes, pH 7.5) with continuous perfusion speed of ~2 ml/min. We used a perfusion valve control system VC-6 (Warner Instruments) for fast local application of modified solutions and drugs as needed (indicated under "Results") at 2 ml/min speed. Low calcium solutions were prepared by adding of Ca^{2+} and EGTA at proportions, calculated with MaxChelator software (Stanford University, Stanford, CA). Required pH of ND96 was adjusted either with NaOH or HCl. The effects of anions (PO_4^{3-}, SO_4^{2-}, and NO_3^-) and inositol polyphosphates were studied by their addition to ND96 with subsequent pH readjustments. High potassium and sodium-free solution (NDX) were prepared by equimolar substitution of sodium with potassium and NMDG, respectively. Phosphate solution was made by mixing of 300 mM stock solutions of mono- and dibasic sodium phosphates until pH 7.4 was obtained.

For the yeast giant vacuole experiments, currents were recorded in whole-vacuole patch-clamp mode. Recording electrodes were prepared as described above and treated with Sigmacote (tip resistance of ~15 MΩ) and then backfilled with recording solution. The recording pipette was applied to the vacuolar membrane for a few minutes to establish gigaseal formation (~10 GΩ). Whole-vacuole configuration was achieved by application of a series of ZAP pulses (1.3 V, 50 ms). Before starting the recording we let the pipette solution diffuse into the vacuole for 5 min. All recordings were performed at $V_h = +60$ mV. An Axopatch 200b amplifier was used for current registration, and the data were filtered at 1000 Hz, digitized with Digidata 1550A (Axon Instruments), and analyzed offline using PClamp 10 software.

Statistical analysis

All of the values are expressed as means ± S.D. unless indicated. Significant differences between treatments were compared using unpaired Student's t tests. Differences were considered statistically significant at $p < 0.05$, and n refers to the number of independent biological experiments performed. All

statistical analyses were conducted using GraphPad Prism 6 (GraphPad Software, San Diego, CA).

Author contributions—E. P., C. D. C., G. H., V. J. S., and R. D. conceptualization; E. P., C. D. C., G. H., V. J. S., and R. D. data curation; E. P., C. D. C., G. H., V. J. S., and R. D. formal analysis; E. P., C. D. C., G. H., V. J. S., and R. D. validation; E. P., C. D. C., G. H., M. S., C. W., A. K. D., H. J. J., V. J. S., and R. D. investigation; E. P., C. D. C., and R. D. visualization; E. P., C. D. C., G. H., M. S., C. W., A. K. D., H. J. J., V. J. S., and R. D. methodology; E. P., H. J. J., and V. J. S. writing-review and editing; V. J. S. and R. D. supervision; R. D. resources; R. D. funding acquisition; R. D. writing-original draft; R. D. project administration.

Acknowledgments—We thank Dr. Shin Hamamoto (Tohoku University, Sendai, Japan) for advice with the giant vacuoles preparation technique and Dr. Keith Gull for pPOTv6 plasmid.

References

1. Rodrigues, C. O., Scott, D. A., and Docampo, R. (1999) Characterization of a vacuolar pyrophosphatase in *Trypanosoma brucei* and its localization to acidocalcisomes. *Mol. Cell. Biol.* **19,** 7712–7723 CrossRef Medline
2. Lander, N., Ulrich, P. N., and Docampo, R. (2013) *Trypanosoma brucei* vacuolar transporter chaperone 4 (TbVtc4) is an acidocalcisome polyphosphate kinase required for *in vivo* infection. *J. Biol. Chem.* **288,** 34205–34216 CrossRef Medline
3. Hothorn, M., Neumann, H., Lenherr, E. D., Wehner, M., Rybin, V., Hassa, P. O., Uttenweiler, A., Reinhardt, M., Schmidt, A., Seiler, J., Ladurner, A. G., Herrmann, C., Scheffzek, K., and Mayer, A. (2009) Catalytic core of a membrane-associated eukaryotic polyphosphate polymerase. *Science* **324,** 513–516 CrossRef Medline
4. Ruiz, F. A., Rodrigues, C. O., and Docampo, R. (2001) Rapid changes in polyphosphate content within acidocalcisomes in response to cell growth, differentiation, and environmental stress in *Trypanosoma cruzi*. *J. Biol. Chem.* **276,** 26114–26121 CrossRef Medline
5. Bru, S., Martínez-Laínez, J. M., Hernández-Ortega, S., Quandt, E., Torres-Torronteras, J., Martí, R., Canadell, D., Ariño, J., Sharma, S., Jiménez, J., and Clotet, J. (2016) Polyphosphate is involved in cell cycle progression and genomic stability in *Saccharomyces cerevisiae*. *Mol. Microbiol.* **101,** 367–380 CrossRef Medline
6. Neef, D. W., and Kladde, M. P. (2003) Polyphosphate loss promotes SNF/SWI- and Gcn5-dependent mitotic induction of PHO5. *Mol. Cell. Biol.* **23,** 3788–3797 CrossRef Medline
7. Yang, Y., Ko, T. P., Chen, C. C., Huang, G., Zheng, Y., Liu, W., Wang, I., Ho, M. R., Hsu, S. T., O'Dowd, B., Huff, H. C., Huang, C. H., Docampo, R., Oldfield, E., and Guo, R. T. (2016) Structures of trypanosome vacuolar soluble pyrophosphatases: antiparasitic drug targets. *ACS Chem. Biol.* **11,** 1362–1371 CrossRef Medline
8. Lemercier, G., Espiau, B., Ruiz, F. A., Vieira, M., Luo, S., Baltz, T., Docampo, R., and Bakalara, N. (2004) A pyrophosphatase regulating polyphosphate metabolism in acidocalcisomes is essential for *Trypanosoma brucei* virulence in mice. *J. Biol. Chem.* **279,** 3420–3425 CrossRef Medline
9. Sethuraman, A., Rao, N. N., and Kornberg, A. (2001) The endopolyphosphatase gene: essential in *Saccharomyces cerevisiae*. *Proc. Natl. Acad. Sci. U.S.A.* **98,** 8542–8547 CrossRef Medline
10. Andreeva, N., Trilisenko, L., Eldarov, M., and Kulakovskaya, T. (2015) Polyphosphatase PPN1 of *Saccharomyces cerevisiae*: switching of exopolyphosphatase and endopolyphosphatase activities. *PLoS One* **10,** e0119594 CrossRef Medline
11. Gerasimaite, R., and Mayer, A. (2017) Ppn2, a novel Zn^{2+}-dependent polyphosphatase in the acidocalcisome-like yeast vacuole. *J. Cell Sci.* **130,** 1625–1636 CrossRef Medline
12. Ravera, S., Virkki, L. V., Murer, H., and Forster, I. C. (2007) Deciphering PiT transport kinetics and substrate specificity using electrophysiology and flux measurements. *Am. J. Physiol. Cell Physiol.* **293,** C606–C620 CrossRef Medline
13. Ferreira, G. C., and Pedersen, P. L. (1993) Phosphate transport in mitochondria: past accomplishments, present problems, and future challenges. *J. Bioenerg. Biomembr.* **25,** 483–492 CrossRef Medline
14. Hürlimann, H. C., Stadler-Waibel, M., Werner, T. P., and Freimoser, F. M. (2007) Pho91 Is a vacuolar phosphate transporter that regulates phosphate and polyphosphate metabolism in *Saccharomyces cerevisiae*. *Mol. Biol. Cell* **18,** 4438–4445 CrossRef Medline
15. Huang, G., Ulrich, P. N., Storey, M., Johnson, D., Tischer, J., Tovar, J. A., Moreno, S. N., Orlando, R., and Docampo, R. (2014) Proteomic analysis of the acidocalcisome, an organelle conserved from bacteria to human cells. *PLoS Pathog.* **10,** e1004555 CrossRef Medline
16. Jimenez, V., and Docampo, R. (2015) TcPho91 is a contractile vacuole phosphate sodium symporter that regulates phosphate and polyphosphate metabolism in *Trypanosoma cruzi*. *Mol. Microbiol.* **97,** 911–925 CrossRef Medline
17. Wild, R., Gerasimaite, R., Jung, J. Y., Truffault, V., Pavlovic, I., Schmidt, A., Saiardi, A., Jessen, H. J., Poirier, Y., Hothorn, M., and Mayer, A. (2016) Control of eukaryotic phosphate homeostasis by inositol polyphosphate sensor domains. *Science* **352,** 986–990 CrossRef Medline
18. Gerasimaite, R., Pavlovic, I., Capolicchio, S., Hofer, A., Schmidt, A., Jessen, H. J., and Mayer, A. (2017) Inositol pyrophosphate specificity of the SPX-dependent polyphosphate polymerase VTC. *ACS Chem. Biol.* **12,** 648–653 CrossRef Medline
19. Albert, C., Safrany, S. T., Bembenek, M. E., Reddy, K. M., Reddy, K., Falck, J., Bröcker, M., Shears, S. B., and Mayr, G. W. (1997) Biological variability in the structures of diphosphoinositol polyphosphates in *Dictyostelium discoideum* and mammalian cells. *Biochem. J.* **327,** 553–560 CrossRef Medline
20. Szczepanska-Konkel, M., Yusufi, A. N., and Dousa, T. P. (1987) Interactions of [^{14}C]phosphonoformic acid with renal cortical brush-border membranes: relationship to the Na^+-phosphate co-transporter. *J. Biol. Chem.* **262,** 8000–8010 Medline
21. Virkki, L. V., B. J. Murer, H., and Forster, I. C. (2007) Phosphate transporters:a tale of two solute carrier families. *Am. J. Physiol. Renal. Physiol.* **293,** F643–F654 CrossRef Medline
22. Villa-Bellosta, R., Levi, M., and Sorribas, V. (2009) Vascular smooth muscle cell calcification and SLC20 inorganic phosphate transporters: effects of PDGF, TNF-α, and P_i. *Pflugers Arch.* **458,** 1151–1161 CrossRef Medline
23. Saliba, K. J., Martin, R. E., Bröer, A., Henry, R. I., McCarthy, C. S., Downie, M. J., Allen, R. J., Mullin, K. A., McFadden, G. I., Bröer, S., and Kirk, K. (2006) Sodium-dependent uptake of inorganic phosphate by the intracellular malaria parasite. *Nature* **443,** 582–585 Medline
24. Yabe, I., Horiuchi, K., Nakahara, K., Hiyama, T., Yamanaka, T., Wang, P. C., Toda, K., Hirata, A., Ohsumi, Y., Hirata, R., Anraku, Y., and Kusaka, I. (1999) Patch clamp studies on V-type ATPase of vacuolar membrane of haploid *Saccharomyces cerevisiae*: preparation and utilization of a giant cell containing a giant vacuole. *J. Biol. Chem.* **274,** 34903–34910 CrossRef Medline
25. Michaillat, L., and Mayer, A. (2013) Identification of genes affecting vacuole membrane fragmentation in *Saccharomyces cerevisiae*. *PLoS One* **8,** e54160 CrossRef Medline
26. Akoda, K., Van den Bossche, P., Lyaruu, E. A., De Deken, R., Marcotty, T., Coosemans, M., and Van den Abbeele, J. (2009) Maturation of a *Trypanosoma brucei* infection to the infectious metacyclic stage is enhanced in nutritionally stressed tsetse flies. *J. Med. Entomol.* **46,** 1446–1449 CrossRef Medline
27. Hartman, M. L., Groppo, F., Ohnishi, M., Goodson, J. M., Hasturk, H., Tavares, M., Yaskell, T., Floros, C., Behbehani, K., and Razzaque, M. S. (2013) Can salivary phosphate levels be an early biomarker to monitor the evolvement of obesity? *Contrib. Nephrol.* **180,** 138–148 CrossRef Medline
28. Desfougères, Y., Gerasimaite, R. U., Jessen, H. J., and Mayer, A. (2016) Vtc5, a novel subunit of the vacuolar transporter chaperone complex, regulates polyphosphate synthesis and phosphate homeostasis in yeast. *J. Biol. Chem.* **291,** 22262–22275 CrossRef Medline

29. Thomas, M. R., and O'Shea, E. K. (2005) An intracellular phosphate buffer filters transient fluctuations in extracellular phosphate levels. *Proc. Natl. Acad. Sci. U.S.A.* **102,** 9565–9570 CrossRef Medline
30. Niyogi, S., Jimenez, V., Girard-Dias, W., de Souza, W., Miranda, K., and Docampo, R. (2015) Rab32 is essential for maintaining functional acidocalcisomes and for growth and infectivity of *Trypanosoma cruzi*. *J. Cell Sci.* **128,** 2363–2373 CrossRef Medline
31. Ramakrishnan, S., Asady, B., and Docampo, R. (2018) Acidocalcisome-mitochondrion membrane contact sites in *Trypanosoma brucei*. *Pathogens* **7,** E33 Medline
32. Cunningham, I. (1977) New culture medium for maintenance of tsetse tissues and growth of trypanosomatids. *J. Protozool.* **24,** 325–329 CrossRef Medline
33. Gietz, R. D., and Schiestl, R. H. (2007) High-efficiency yeast transformation using the LiAc/SS carrier DNA/PEG method. *Nat. Protoc.* **2,** 31–34 CrossRef Medline
34. Aslett, M., Aurrecoechea, C., Berriman, M., Brestelli, J., Brunk, B. P., Carrington, M., Depledge, D. P., Fischer, S., Gajria, B., Gao, X., Gardner, M. J., Gingle, A., Grant, G., Harb, O. S., Heiges, M., *et al.* (2010) TriTrypDB: a functional genomic resource for the Trypanosomatidae. *Nucleic Acids Res.* **38,** D457–D462 CrossRef Medline
35. Dean, S., Sunter, J., Wheeler, R. J., Hodkinson, I., Gluenz, E., and Gull, K. (2015) A toolkit enabling efficient, scalable and reproducible gene tagging in trypanosomatids. *Open Biol.* **5,** 140197 CrossRef Medline
36. Ulrich, P. N., Lander, N., Kurup, S. P., Reiss, L., Brewer, J., Soares Medeiros, L. C., Miranda, K., and Docampo, R. (2014) The acidocalcisome vacuolar transporter chaperone 4 catalyzes the synthesis of polyphosphate in insect-stages of *Trypanosoma brucei* and *T. cruzi*. *J. Eukaryot. Microbiol.* **61,** 155–165 CrossRef Medline
37. Lanzetta, P. A., Alvarez, L. J., Reinach, P. S., and Candia, O. A. (1979) An improved assay for nanomole amounts of inorganic phosphate. *Anal. Biochem.* **100,** 95–97 CrossRef Medline
38. Díaz, P., Vallejos, C., Guerrero, I., and Riquelme, G. (2008) Barium, TEA and sodium sensitive potassium channels are present in the human placental syncytiotrophoblast apical membrane. *Placenta* **29,** 883–891 CrossRef Medline